Article

Discovery Medicine 2026; 38(211): 2664–2674
https://doi.org/10.24976/Discov.Med.202638211.209

FTO/EFNB2 Axis Protects Retinal Ganglion Cells Against H_2O_2-Induced Oxidative Damage

Yi Yin[1], Zhaoyang Meng[1], Yu Wang[1], Binbin Zhan[1], Yan Zhang[2,*], Zhenxi Xia[3,*]

[1]Department of Ophthalmology, Beijing Friendship Hospital, Capital Medical University, 100050 Beijing, China
[2]Department of Ophthalmology, The Seventh Medical Center of PLA General Hospital, 100700 Beijing, China
[3]Department of Neurology, The Seventh Medical Center of PLA General Hospital, 100700 Beijing, China
*Correspondence: iamyanzi_1972@163.com (Yan Zhang); xzxlzdx@sina.com (Zhenxi Xia)
Submitted: 25 May 2026 Revised: 3 July 2026 Accepted: 15 July 2026 Published: 24 August 2026

Background: Traumatic optic neuropathy (TON) causes progressive retinal ganglion cell (RGC) loss and oxidative injury, leading to visual dysfunction. Ephrin B2 (EFNB2) is elevated in optic nerve injury; however, it is unclear how the fat mass and obesity-associated gene (FTO) regulates it upstream. This study examined whether RGCs are shielded from hydrogen peroxide (H_2O_2)-induced oxidative damage through FTO-mediated EFNB2 overexpression.

Methods: Primary RGCs were isolated and exposed to H_2O_2 to establish an *in vitro* oxidative stress injury model. We first verified the concentration-dependent induction of FTO and EFNB2 by H_2O_2. Gain- and loss-of-function assays were performed using FTO overexpression and knockdown plasmids to assess its effects on RGC viability, apoptosis, reactive oxygen species (ROS) accumulation, caspase-3 activity, and the expression of EFNB2, erythropoietin-producing hepatoma receptor B4 (EPHB4) and apoptosis-related proteins. Rescue experiments with EFNB2 knockdown were further conducted to confirm whether EFNB2 acts as a downstream effector of FTO.

Results: H_2O_2 treatment elevated FTO and EFNB2 expression in RGCs in a concentration-dependent manner ($p < 0.01$). FTO overexpression alleviated H_2O_2-induced reductions in cell viability, as well as increases in apoptosis, caspase-3 activation, and ROS levels ($p < 0.001$), while FTO knockdown exacerbated these injuries ($p < 0.001$). Moreover, FTO overexpression enhanced EFNB2 and EPHB4 expression, and suppressed Bax and cleaved caspase-3 levels ($p < 0.001$). Knockdown of EFNB2 reversed the protective effects of FTO overexpression on RGC survival, oxidative stress, and apoptosis ($p < 0.001$).

Conclusions: FTO upregulates EFNB2 and EPHB4 expression, reduces ROS and apoptosis, and is associated with the protection of RGCs against H_2O_2-induced oxidative damage. The FTO/EFNB2 axis may represent a protective mechanism against oxidative damage in RGCs *in vitro*, warranting further investigation in traumatic optic neuropathy models.

Keywords: fat mass- and obesity-associated gene; EFNB2; TON; RGC; hydrogen peroxide; cell damage; apoptosis

Introduction

Traumatic optic neuropathy (TON) is known as a vision-threatening condition caused by direct or indirect trauma, including head injuries, assaults, road accidents or disasters [1,2]. TON is uncommon in the general population, but young men face increased risk; among recent combat veterans with orbital fractures, its incidence approaches 50% [3]. TON contributes to optic nerve edema and disrupts the pial vessels, leading to vascular supply limitation [4,5]. Secondary damage to the optic nerve is caused by an inflammatory response triggered by the above events, which results in axonal degeneration and retinal ganglion cells (RGCs) death [2,4]. RGCs play an important role in vision, and their damage can lead to permanent blindness, as observed in advanced glaucoma [6]. Emerging evidence has further elucidated the complex pathological mechanisms underlying TON. Oxidative stress, characterized by excessive reactive oxygen species (ROS) and hydrogen peroxide (H_2O_2) accumulation, is a key driver of RGC injury [7,8]. Ferroptosis, along with apoptosis, pyroptosis, and necroptosis, has been implicated at different stages of TON [9,10]. Neuroinflammation also plays a pivotal role, with microglia orchestrating inflammatory responses following optic nerve injury [11]. Additionally, N6-methyladenosine (m6A) RNA methylation has emerged as a crucial epigenetic regulator in TON, with fat mass and obesity-associated gene (FTO) functioning as a key m6A demethylase [12]. Therefore, developing effective therapeutic strategies to protect RGCs from injury is needed.

Ephrin B (EFNB) is closely associated with various developmental processes regulated by cell-cell contact, including synaptic plasticity and neural development, as well as pathological processes such as neurodegeneration and cancer [13,14]. The *EFNB2* gene, which is a membrane-anchored ligand belonging to the largest family of receptor tyrosine kinases [15], is involved in mediating developmental processes, particularly the development of the ner-

vous system and erythrocytes, according to the GeneCard database. Strong et al. [16] reported that EFNB2 phosphorylation was increased after optic nerve injury. EFNB2 acts as a ligand for erythropoietin-producing hepatoma receptor B (EPHB) receptors, forming bidirectional Ephrin-EphR signaling [17], and is involved in neurodevelopment, neuronal migration, erythropoiesis, and angiogenesis [18]. Nevertheless, few studies have investigated how EFNB2 participates in RGCs.

Neural stem cell self-renewal and differentiation are tightly linked to N6-methyladenosine (m6A) alteration, and m6A RNA methylation is crucial to the pathological process following TON [19]. A previous study found that four genes associated with up-regulated m6A methylation—methyltransferase-like 3 (METTL3) [20], Wilms' tumor suppressor-1-associated protein (WTAP), FTO, and ALKBH5—might have EFNB2 modification sites based on prediction [21]. We expected that m6A-associated proteins could enhance EFNB2 expression through demethylation. METTL3 and WTAP mediate m6A methylation whereas FTO mediates m6A demethylation [12,20,22]. Moreover, the mRNA demethylase FTO has been found to up-regulate the m6A level of EFNB2 mRNA [23]. Accordingly, only FTO was within our selection range. Previous studies have demonstrated the widespread expression and high enrichment of FTO in neurons in the brain [24]. Research has demonstrated that the loss of FTO leads to a reduction in brain volume and weight, while also reducing the proliferation and neuronal differentiation of neural stem cells [25]. However, it remains unclear whether FTO loss causes optic nerve injury. The FTO-related mechanism regulating EFNB2 in RGCs also remains obscure.

Here, we first investigated the role of FTO in RGC injury and then examined the involvement of EFNB2 in FTO-mediated effects on RGCs.

Materials and Methods

RGCs Isolation and Culture

Pregnant Sprague-Dawley (SD) rats (n = 5) at gestational days 19–21 were obtained from Hangzhou Medical College (China). After natural delivery, male neonatal rats (n = 30) at postnatal days 1–3 were selected for RGC isolation. Sex was determined by anogenital distance and confirmed by gonadal morphology. Only male rats were used to avoid potential confounding effects of female hormonal cycles on oxidative stress responses [26]. Neonatal rats were housed under standard conditions (22 ± 1 °C, 50%–55% humidity, 12 h light/dark cycle).

Rats were anesthetized with sodium pentobarbital (40 mg/kg, i.p.; P3761, Sigma-Aldrich, St. Louis, MO, USA) and euthanized by cervical dislocation. Neonatal rats (postnatal days 1–3) were anesthetized by hypothermia using an insulating barrier to avoid direct contact with ice or pre-cooled surfaces (surface temperature 2–3 °C) for approximately 5–8 minutes. Anesthesia depth was confirmed by loss of consciousness and absence of withdrawal reflexes to toe pinch. After cervical dislocation, death was confirmed by respiratory arrest, absence of heartbeat, and dilated pupils unresponsive to light. All procedures were performed by trained personnel following the standardized operating procedures approved by the Institutional Animal Care and Use Committee (IACUC). In a sterile environment, the eyeballs of SD rats were removed after the rats were immersed in 75% alcohol (E299578, Aladdin, Shanghai, China). Phosphate-buffered saline (PBS, PB180327, Procell, Wuhan, China) with 1% penicillin-streptomycin (15070063, Thermo Fisher, Waltham, MA, USA) was used to wash the isolated eyeballs three times. Under a light microscope (WMS-1033, WUMO, Shanghai, China), retinal tissues were separated, cleaned with PBS, chopped into tiny pieces, and digested for 20 minutes at 37 °C in a 5% CO_2 incubator using 1.25 g/L trypsin (T274333, Aladdin, Shanghai, China). Dulbecco's modified Eagle's medium/F12 (DMEM/F12, D0697, Sigma-Aldrich, St. Louis, MO, USA) supplemented with 10% fetal bovine serum (FBS, C0227, Beyotime, Shanghai, China) was used to halt the digestion process.

The cell pellet was resuspended in DMEM/F12 supplemented with 10% FBS for cell isolation after centrifugation for 10 minutes. For macrophage depletion, cells were incubated with CD11b/c antibody (ab1211, Abcam) at 4 °C for 30 min, followed by Dynabeads™ Sheep Anti-mouse IgG at 4 °C for 30 min. Bead-bound cells were removed using a magnetic separator. The cell suspension were incubated with PE-conjugated anti-Thy1.1 antibody (ab95812, Abcam, Cambridge, UK) at 4 °C for 30 min, followed by anti-PE magnetic beads at 4 °C for 30 min. RGC-coated magnetic beads were collected magnetically, washed three times with sorting buffer, and resuspended in complete culture medium After RGC purification using anti-Thy1.1 antibody, mycoplasma testing (C0296, Beyotime, Shanghai, China) was performed and yielded negative results throughout the culture period. The purified RGCs were seeded in 25-cm^2 poly-D-lysine-coated flasks (CLS430372, Sigma-Aldrich, St. Louis, MO, USA) and cultured in DMEM/F12 supplemented with 10 ng/mL ciliary neurotrophic factor (HY-P7147, MCE, Monmouth Junction, NJ, USA), 50 ng/mL brain-derived neurotrophic factor (RP10917, Thermo Fisher, Massachusetts, USA), 5 ng/mL basic fibroblast growth factor (5414, CST, Danvers, Massachusetts, USA), 10 µM forskolin (IF0200, Solarbio, Beijing, China), and 5 µg/mL insulin (I8040, Solarbio, Beijing, China). The medium was replaced every two days, and the cells were kept at 37 °C in a humidified 5% CO_2 environment [27].

Immunofluorescence Identification of RGCs

To verify the identity of the isolated RGCs, immunofluorescence staining was performed using the RGC-

specific marker RBPMS. Briefly, cultured cells were fixed with 4% paraformaldehyde (C0222, Beyotime, Shanghai, China) for 15 min at room temperature, permeabilized with 0.3% Triton X-100 (ST1723-100ml, Beyotime, Shanghai, China) for 10 min, and blocked with 5% bovine serum albumin (BSA) for 1 h. The cells were then incubated overnight at 4 °C with anti-RBPMS antibody (ab152101, 1:500, Abcam, Waltham, MA, USA). After washing with PBS, cells were incubated with the corresponding fluorescent secondary antibody (ab150077, 1:200, Abcam, Waltham, MA, USA) for 1 h at room temperature in the dark. Nuclei were counterstained with DAPI (40728ES03, Yeasen, Shanghai, China) for 5 min.

RGCs Treatment and Transfection

After being cultured in a 96-well plate (CLS3922, Sigma-Aldrich, St. Louis, MO, USA) for 24 h, RGCs received gradually increasing concentrations (0, 100, 200, 300, 400 µmol/L) of hydrogen peroxide (H_2O_2, H112519, Aladdin, Shanghai, China) for 12 h. H_2O_2 at 300 µM was applied to treat RGCs in subsequent experiments [28]. For transfection, plasmids overexpressing FTO (pRP[Exp]-EGFP/Puro-CAG>rFto[NM_001039713.1]), short hairpin RNA against EFNB2 (shEFNB2, pPB[shRNA]-EGFP/Puro-U6>rEfnb2[shRNA#1], VectorBuilder, Guangzhou, China, target sequence: AGCCGACAGATGCACTATTAA) and the empty vectors (negative control (NC), shNC, target sequence: CCTAAGGTTAAGTCGCCCTCG) were provided by VectorBuilder (Guangzhou, China). Small interfering RNA against FTO (siFTO-1, siB160927091346-1-5, CGATACAAACTTTGCACCGAT; siFTO-2, siB160927091631-1-5, GTCTCGTTGAAATCCTTTGAT; siFTO-3, siB160927101416-1-5, CCAGGGAGACTGCTATTTCAT) and the empty vectors (siNC, siN0000002-1-5, target sequence: ACGUGACACGUUCGGAGAATT) were provided by RIBOBIO (Guangzhou, China). When a 70%–90% cell confluence was reached, RGCs were transfected with siFTO, siNC, plasmids overexpressing FTO, NC, shEFNB2 or shNC using Lipofectamine™ 3000 Transfection Reagent (L3000015, Thermo Fisher, Waltham, MA, USA) in the presence or absence of H_2O_2.

Quantitative Real-Time Polymerase Chain Reaction (qRT-PCR)

Total RNA was extracted from RGCs with TRIzol reagent (93289, Sigma-Aldrich, St. Louis, MO USA). RNA concentration was quantified by a UV spectrophotometer (DR6000, HACH, Loveland, CO, USA). cDNA was synthesized from RNA using SuperScript™ IV reverse transcriptase (18090010, Thermo Fisher, Waltham, MA, USA) according to the manufacturer's protocol. Real-time PCR was carried out with SYBR Premix Ex Taq II (RR820A, Takara, Kusatsu, Shiga, Japan) on the CFX Connect™ system (1855201, Bio-Rad, Hercules, CA, USA). Table 1 contains primer sequence information. The relative expression was calculated using the $2^{-\Delta\Delta ct}$ method and normalized to β-actin expression [29].

Western Blot Analysis

FTO, EFNB2, EPHB4, Bcl-2 associated X (Bax), and cleaved caspase-3 expression in RGCs were detected by Western blotting. RIPA lysis buffer (20-188, Sigma-Aldrich, St. Louis, MO, USA) was used to extract total proteins, which were then measured using the BCA Protein Assay Kit (7780S, CST, Danvers, MA, USA). Protein samples were transferred to PVDF membranes (88585, Thermo Fisher, Waltham, MA, USA) after being separated by SDS-PAGE (P1040, Solarbio, Beijing, China). After blocking the membranes with 5% non-fat milk for 1 h, they were treated with primary antibodies (Table 2) at 4 °C for a whole night, and then incubated with secondary antibodies (Table 2) for 1 h at room temperature. Protein bands were quantified using the FluorChem M imaging equipment (Protein Simple, San Jose, CA, USA) and visualized with chemiluminescent substrate (34577, Thermo Fisher, Waltham, MA, USA) using β-actin as an internal reference.

3-(4,5-Dimethylthiazol-2-yl)-2,5-diphenyl-2H-tetrazolium Bromide (MTT) Assay

RGC viability after transfection and H_2O_2 treatment was assessed by MTT assay. RGCs were seeded in 96-well plates at 5×10^3 cells/well and cultured for 48 h. After PBS washing, 10 µL MTT solution (M8180, Solarbio, Beijing, China, 5 mg/mL) was added and incubated for 4 h. The medium was then removed, 100 µL DMSO (D8370, Solarbio, Beijing, China) was added, and absorbance at 570 nm was measured using a Bio-Rad (Hercules, CA, USA) 680 microplate reader.

Flow Cytometry Assay

RGC apoptosis was assessed using an apoptosis kit (A211-01, Vazyme, Nanjing, China). Following transfection and H_2O_2 treatment, 1×10^6 RGCs were collected, rinsed with PBS (C0221A, Beyotime, Shanghai, China), then resuspended in 250 µL binding solution. Following a 15 min dark incubation period at room temperature with 5 µL annexin fluorescein isothiocyanate (FITC) and 10 µL propidium iodide (PI), the cells were diluted with 500 µL binding buffer and analyzed using Attune NxT flow cytometry (A24860, Thermo Fisher, Waltham, MA, USA). FlowJo software (Becton-Dickinson, Franklin Lakes, NJ, USA) was used to calculate apoptosis rates.

The DCFH-DA probe (HY-D0940, MedChemExpress (MCE), Monmouth Junction, NJ, USA) was used to assess intracellular ROS levels. Trypsin (T1426; P2714, Sigma-Aldrich, St. Louis, MO, USA) was used to digest RGCs. Cell pellets were collected following centrifugation for 5 min at 1500 rpm in D-Hanks (H1045, Solarbio, Beijing, China). After 30 min of incubation with 10 µM DCFH-DA

Table 1. Gene sequence primers.

Name	Forward primer (5′-3′)	Reverse primer (5′-3′)
FTO	GGGAGCGGGAAGCTAAGAA	CAGCCTCTCGGAAAACCAGT
EFNB2	CAGCCCTAACCTCTGGGGTC	GGCCCTCCAAAGACCCATTTG
β-actin	CTGTGTGGATTGGTGGCTCT	AGCTCAGTAACAGTCCGCC

FTO, fat mass and obesity-associated gene; EFNB2, Ephrin B2.

Table 2. Antibodies used in this study.

Name	Catalog	Molecular weight	Dilution	Manufacturer
FTO	ab280081	58 kDa	1/1000	Abcam, UK
EFNB2	sc-398735	36 kDa	1/1000	Santa Cruz Biotechnology, USA
EPHB4	sc-130081	120 kDa	1/1000	Santa Cruz Biotechnology, USA
Bax	ab32503	21 kDa	1/2000	Abcam, UK
Cleaved caspase-3	#9664	17 kDa	1:1000	CST, USA
β-actin	#4970	45 kDa	1/1000	CST, USA
Goat anti-mouse	ab6789	—	1/2000	Abcam, UK
Goat anti-rabbit	ab205718	—	1/2000	Abcam, UK

EPHB4, erythropoietin-producing hepatoma receptor B4; Bax, Bcl-2 associated X.

(37 °C) in the dark, the cells were washed and analyzed using Attune NxT flow cytometry. Data were processed using FlowJo software.

Caspase-3 Activity Assay

RGCs were seeded in 6-well plates (140675, Thermo Fisher, Waltham, MA, USA) at 2×10^5 cells/mL and treated accordingly. Cells were harvested, centrifuged at 600 g for 5 min at 4 °C, then lysed on ice for 15 min. After centrifugation, the supernatant was collected. A mixture of 40 µL buffer, 50 µL supernatant and 10 µL Ac-DEVD-pNA (2 mM) (C1116, Beyotime, Shanghai, China) was incubated at 37 °C for 2 h, and absorbance at 405 nm was detected.

Statistical Analysis

The data are expressed as mean differences ± standard deviation. The normality of the data was confirmed using the Shapiro–Wilk test before statistical analysis. Graphpad 8.0 (Graphpad Software, CA, USA) was used for statistical analysis. Independent-samples *t*-test was used to compare two groups, and one-way analysis of variance was employed to evaluate results across multiple groups, followed by Tukey's post-hoc test for multiple comparisons. *p* values < 0.05 were regarded as statistically significant.

Results

H_2O_2 Induced the Expression Levels of FTO and EFNB2 in RGCs

To confirm the identity of isolated RGCs, immunofluorescence staining was performed. Immunofluorescence staining showed that the isolated cells were positive for the RGC-specific marker RBPMS (Fig. 1A), confirming the identity of the RGC culture. Then, we used qRT-PCR and Western blotting to examine the effects of various H_2O_2 concentrations (0, 100, 200, 300, and 400 µM) on the relative mRNA and protein expression levels of FTO and EFNB2 in RGCs (Fig. 1B–D, $p < 0.01$). The experimental results showed that H_2O_2 induced the expression levels of FTO and EFNB2 in RGCs in a concentration-dependent manner (Fig. 1B–D, $p < 0.01$).

FTO Overexpression Attenuated H_2O_2-Induced Oxidative Injury in RGC Damage While FTO Silencing Exerted the Opposite Effect

We first evaluated the transfection efficiency of plasmids overexpressing FTO and siFTO (siFTO-1, siFTO-2 and siFTO-3) in RGCs using qRT-PCR and Western blotting. Transfection with all three siFTO constructs reduced FTO expression, with siFTO-3 showing the strongest effect; therefore, siFTO-3 was used in subsequent experiments (Fig. 1E,G,H, $p < 0.05$). Additionally, FTO expression in RGCs was promoted after transfection with plasmids overexpressing FTO (Fig. 1F,I,J, $p < 0.001$). To evaluate how FTO affected H_2O_2-induced changes in RGC viability, an MTT assay was performed, and the results showed that FTO overexpression attenuated the inhibitory effect of H_2O_2 on RGC viability while FTO knockdown further promoted the effect of H_2O_2 (Fig. 2A, $p < 0.001$). H_2O_2 treatment induced RGC apoptosis, and FTO overexpression mitigated the role of H_2O_2, which was promoted by FTO silencing (Fig. 2B,C, $p < 0.001$). Furthermore, the H_2O_2-induced increase in caspase-3 activity in RGCs was attenuated by FTO overexpression and further boosted by FTO knockdown (Fig. 2D, $p < 0.001$). FTO overexpression decreased ROS fluorescence intensity, promoted by H_2O_2 treatment, whereas FTO silencing exerted the opposite effect (Fig. 2E,F, $p < 0.001$). We further explored how FTO influenced the effect of H_2O_2 on EFNB2 expression

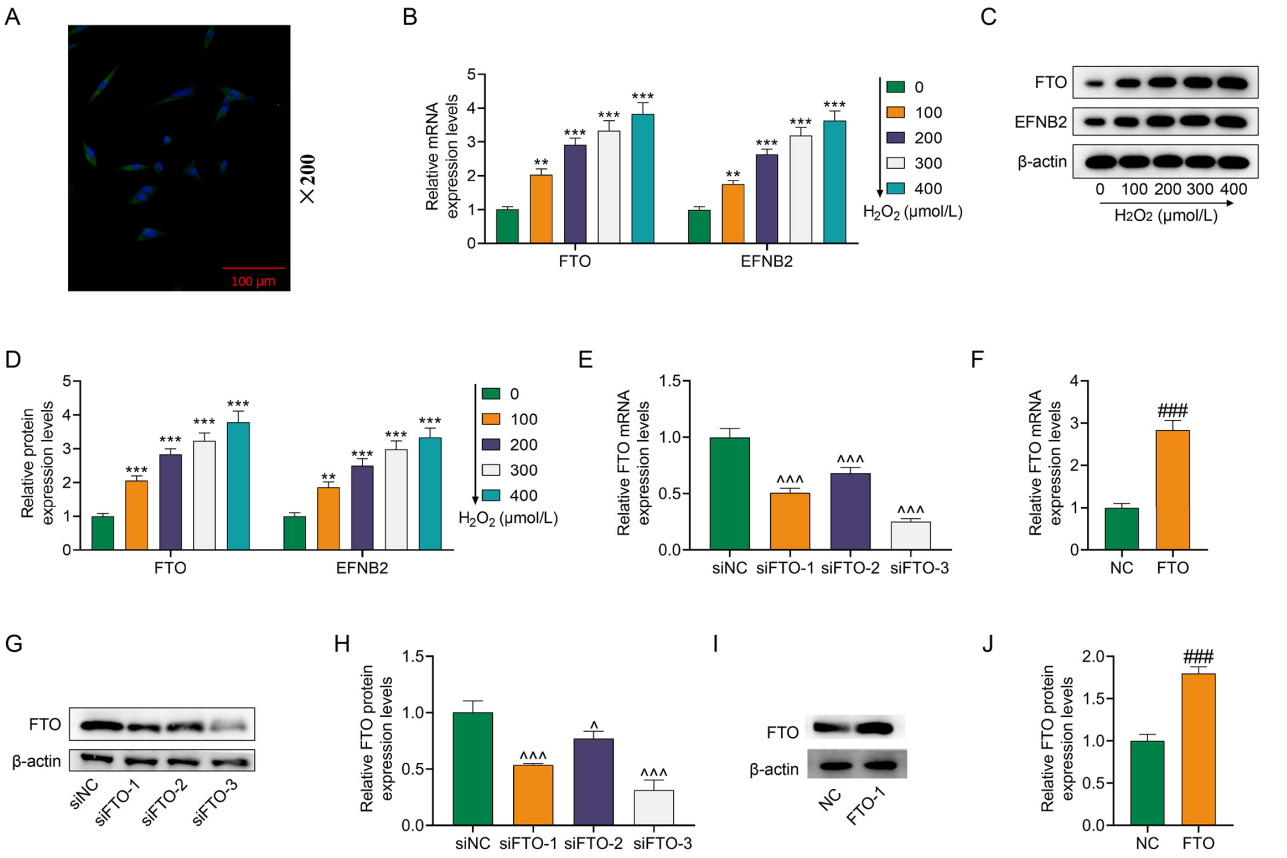

Fig. 1. H_2O_2 induced the expression levels of FTO and EFNB2 in RGCs. (A) Representative immunofluorescence image showing that the isolated cells were positive for the RGC-specific marker RBPMS (green). Nuclei were counterstained with DAPI (blue). (B–D) The expression levels of FTO and EFNB2 in RGCs after treatment with gradually increasing concentrations (0, 100, 200, 300, 400 μM) of H_2O_2 were analyzed using qRT-PCR and Western blotting with β-actin as an internal standard. (E,F) FTO expression in RGCs after transfection with siNC, siFTO (siFTO-1, siFTO-2 or siFTO-3), NC or plasmids overexpressing FTO was detected using qRT-PCR with β-actin serving as a reference gene. (G–J) FTO expression in RGCs after transfection with siNC, siFTO (siFTO-1, siFTO-2 or siFTO-3), NC or plasmids overexpressing FTO was detected using Western blotting, with β-actin serving as a reference gene. Data are presented as mean ± SD (n = 3 independent experiments). $^{**}p < 0.01$, $^{***}p < 0.001$ vs. 0; $^{\wedge}p < 0.05$, $^{\wedge\wedge\wedge}p < 0.001$ vs. siNC; $^{\#\#\#}p < 0.001$ vs. NC. FTO, fat mass- and obesity-associated gene; EFNB2, ephrin B2; RGCs, retinal ganglion cells; H_2O_2, hydrogen peroxide; qRT-PCR, quantitative real-time polymerase chain reaction; DAPI, 4',6-diamidino-2-phenylindole; NC, Negative Control.

in RGCs (Fig. 2G, $p < 0.001$). H_2O_2 enhanced EFNB2 expression, which was further increased by FTO overexpression but reversed by FTO knockdown (Fig. 2G, $p < 0.001$). Collectively, these results demonstrated that FTO overexpression attenuated H_2O_2-induced RGC damage, whereas FTO silencing exerted the opposite effect.

EFNB2 Knockdown Abolished the Protective Effects of FTO Overexpression on RGC Viability and Apoptosis

To explore how EFNB2 participated in the mechanism of FTO action in RGCs, we first analyzed EFNB2 expression after transfection with shEFNB2, and found that shEFNB2 decreased the mRNA and protein levels of EFNB2 (Fig. 3A–C, $p < 0.01$). Then, RGC viability after treatment and transfection was detected using an MTT assay (Fig. 3D, $p < 0.001$). The experimental results showed that FTO overexpression promoted RGC viability suppressed by H_2O_2, whereas knocking down EFNB2 enhanced the effect of H_2O_2 and reversed the role of FTO overexpression (Fig. 3D, $p < 0.001$). H_2O_2 treatment induced RGC apoptosis, which was mitigated by FTO overexpression and further promoted by EFNB2 knockdown (Fig. 3E,F, $p < 0.001$). Furthermore, the effect of FTO overexpression was reversed by EFNB2 knockdown (Fig. 3E,F, $p < 0.001$).

EFNB2 Knockdown Reversed the Effects of FTO Overexpression on ROS Level and Apoptosis-Related Protein Expression

Furthermore, FTO overexpression reduced the ROS fluorescence intensity promoted by H_2O_2 treatment,

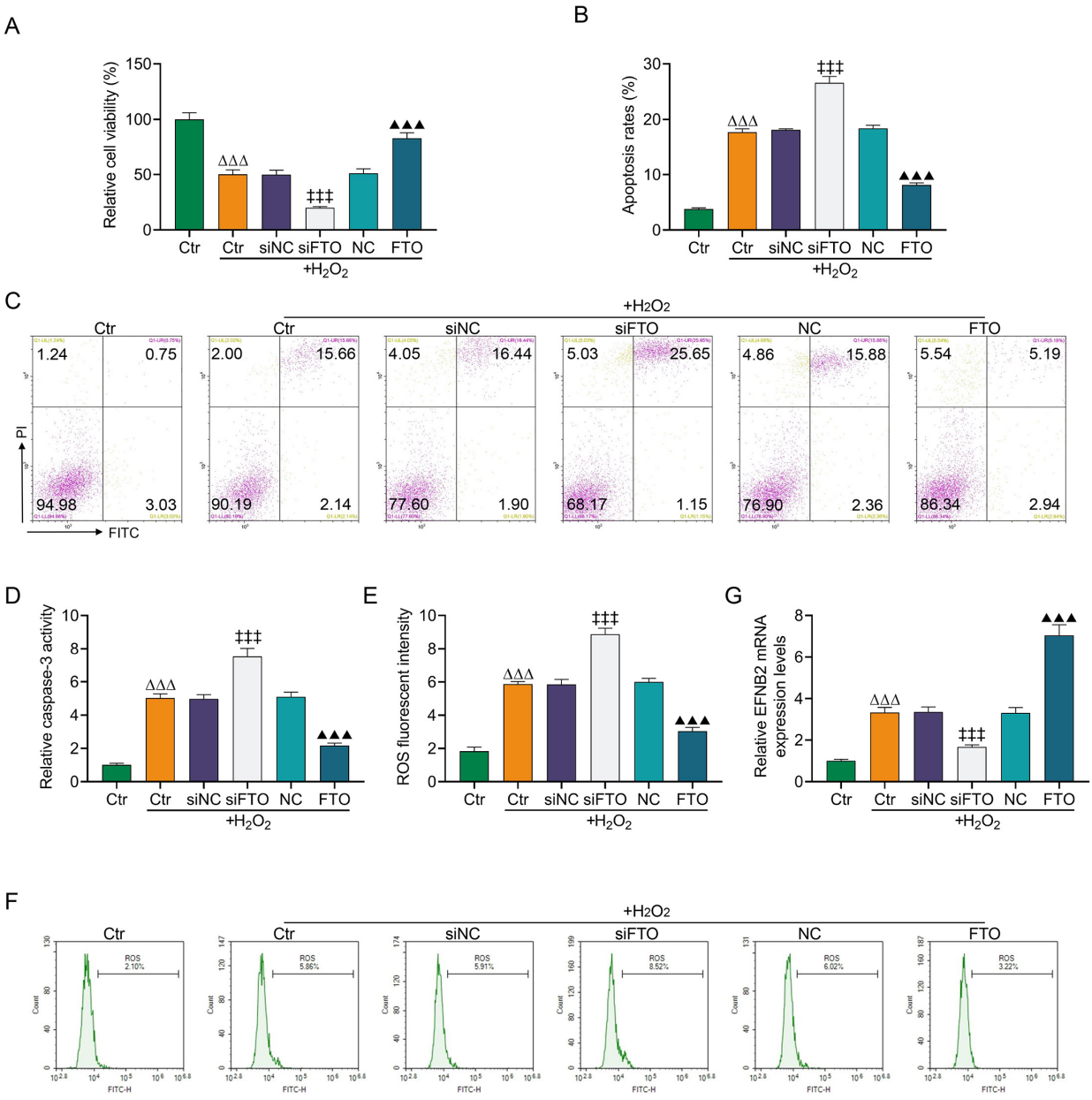

Fig. 2. FTO overexpression attenuated H_2O_2-induced RGC damage while FTO silencing exerted the opposite effect. (A–G) RGCs were divided into six groups: Ctr, Ctr+H_2O_2, H_2O_2+siNC, H_2O_2+siFTO, H_2O_2+NC, H_2O_2+FTO. (A) MTT assay was employed to examine RGC viability following treatment and transfection. (B,C) The apoptotic rate of RGCs in each group was measured by flow cytometry assay. (D) Caspase-3 activity in RGCs was evaluated using a caspase-3 activity assay kit. (E,F) Flow cytometry assay was used to detect ROS fluorescence intensity in RGCs of each group. (G) EFNB2 expression in RGCs was analyzed using qRT-PCR, with β-actin used as the reference gene. Data are presented as mean ± SD (n = 3 independent experiments). $^{\Delta\Delta\Delta}p < 0.001$ vs. Ctr; $^{\ddagger\ddagger\ddagger}p < 0.001$ vs. H_2O_2+siNC; $^{\blacktriangle\blacktriangle\blacktriangle}p < 0.001$ vs. H_2O_2+NC. FTO, fat mass- and obesity-associated gene; RGCs, retinal ganglion cells; siFTO, small interfering RNA against FTO; qRT-PCR, quantitative real-time polymerase chain reaction; Ctr, control; H_2O_2, hydrogen peroxide; MTT, 3-(4,5-dimethylthiazol-2-yl)-2,5-diphenyl-2H-tetrazolium bromide; ROS, reactive oxygen species; EFNB2, ephrin B2; NC, Negative Control.

whereas EFNB2 knockdown further enhanced the effect of H_2O_2 and reversed the effect of FTO overexpression (Fig. 4A,B, $p < 0.001$). Finally, we examined the expression levels of apoptosis-associated proteins and EPHB4 in RGCs using Western blotting. H_2O_2 treatment enhanced EPHB4, Bax and cleaved caspase-3 expression levels, and FTO overexpression further promoted the role of H_2O_2 in EPHB4 and reversed its effect on Bax and cleaved caspase-

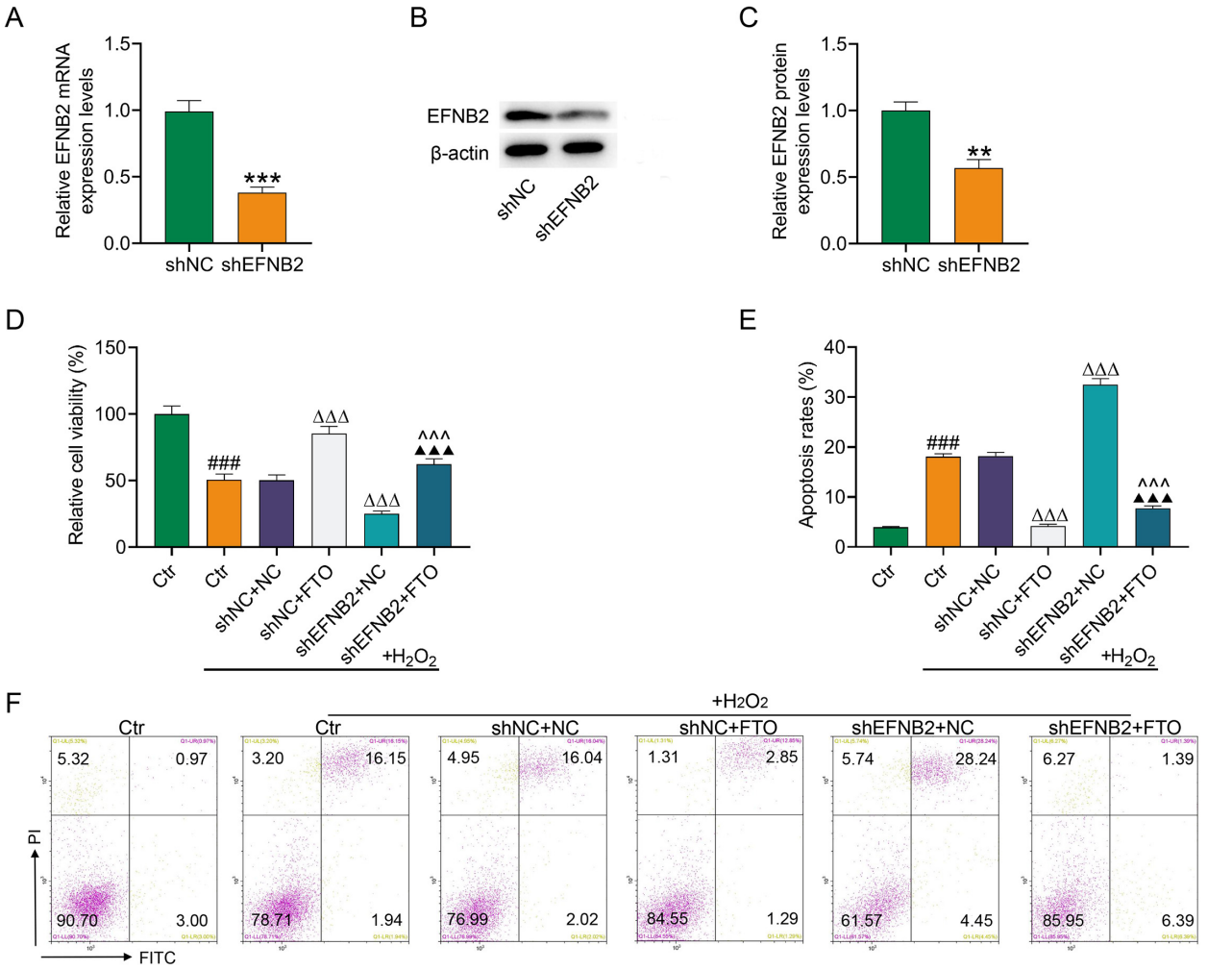

Fig. 3. FTO protects RGCs by upregulating EFNB2 expression: effects on cell viability and apoptosis. (A–C) EFNB2 expression in RGCs treated with shNC or shEFNB2 was analyzed using qRT-PCR and Western blotting. (D–F) RGCs were divided into six groups: Ctr, Ctr+H_2O_2, H_2O_2+shNC+NC, H_2O_2+shNC+FTO, H_2O_2+shEFNB2+NC, H_2O_2+shEFNB2+FTO. (D) RGC viability after treatment and transfection was assessed using an MTT assay. (E,F) Flow cytometry assay was used to measure the apoptotic rate of RGCs. Data are presented as mean ± SD (n = 3 independent experiments). $^{**}p < 0.01$, $^{***}p < 0.001$ vs. shNC; $^{\#\#\#}p < 0.001$ vs. Ctr; $^{\Delta\Delta\Delta}p < 0.001$ vs. H_2O_2+shNC+NC; $^{\wedge\wedge\wedge}p < 0.001$ vs. H_2O_2+shEFNB2+NC; $^{\blacktriangle\blacktriangle\blacktriangle}p < 0.001$ vs. H_2O_2+shNC+FTO. EFNB2, ephrin B2; RGCs, retinal ganglion cells; shEFNB2, short hairpin RNA against EFNB2; qRT-PCR, quantitative real-time polymerase chain reaction; Ctr, control; H_2O_2, hydrogen peroxide; FTO, fat mass- and obesity-associated gene; MTT, 3-(4,5-dimethylthiazol-2-yl)-2,5-diphenyl-2H-tetrazolium bromide; NC, Negative Control.

3, whereas EFNB2 knockdown exerted opposite effects (Fig. 4C,D, $p < 0.001$). Additionally, EFNB2 knockdown counteracted the effects of FTO overexpression (Fig. 4C,D, $p < 0.001$). Together, these experiments suggested that FTO protected RGCs by promoting EFNB2 expression.

Discussion

In the retina, photoreceptors capture light signals and transmit visual information to RGCs via interneurons; RGC axons then form the optic nerve and project to the brain [30]. RGC loss causes severe visual impairment in glaucoma and Leber's hereditary optic neuropathy [31]. Oxidative stress involving excessive ROS and H_2O_2 is a key driver of RGC injury and death [8]. In this study, H_2O_2 treatment reduced RGC viability, increased apoptosis, caspase-3 activity, ROS levels, and expression of Bax and cleaved caspase-3, highlighting the successful induction of RGC damage.

Inhibition of methyltransferase-like 3 (Mettl3)-mediated m6A modification of Hydroxyl-3-methylglutaryl-Coenzyme A synthase 1 (HMGCS1) regulates ferroptosis and has been shown to protect retinal ganglion cells against glutamate excitotoxicity in glaucom [10]. For example, crocin alleviates retinal ischemia-reperfusion-triggered

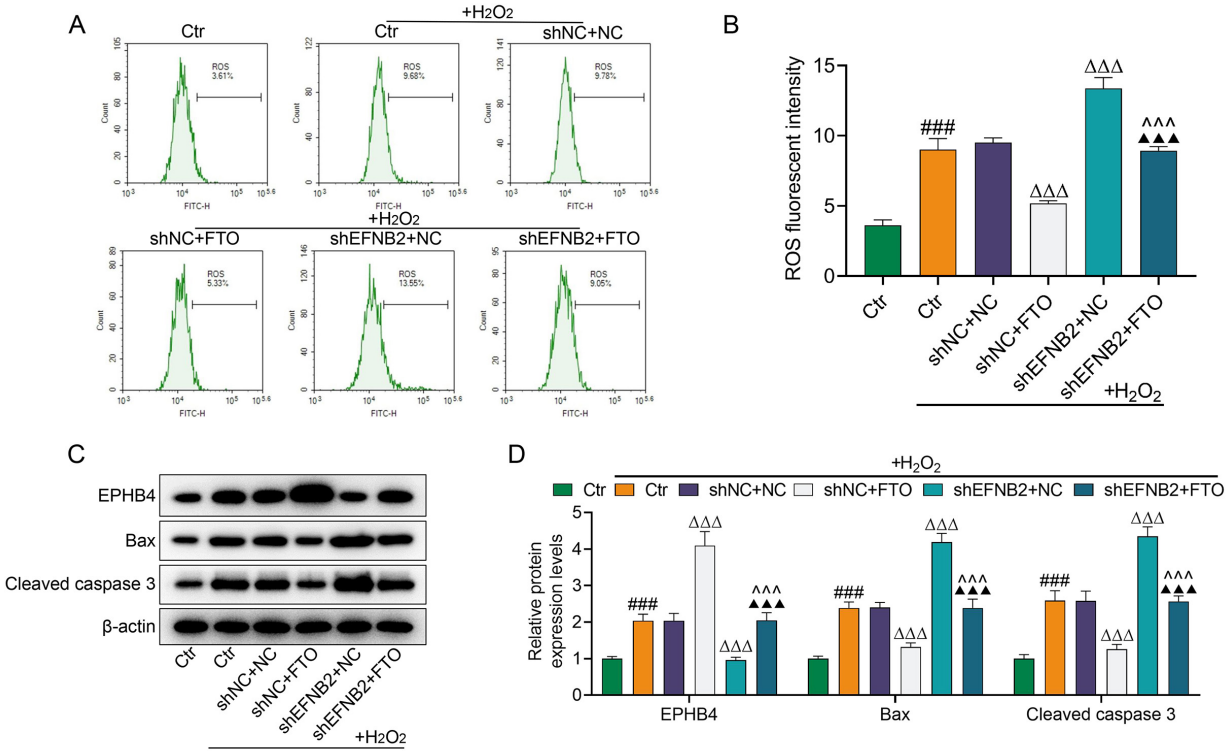

Fig. 4. FTO regulates ROS levels and apoptosis-related protein expression via EFNB2 in RGCs. (A,B) ROS fluorescence intensity in RGCs of each group was detected by flow cytometry assay. (C,D) The expression levels of apoptosis-associated proteins, including Bax and cleaved caspase-3, and EPHB4 in RGCs were examined using Western blotting, with β-actin used as an internal standard. Data are presented as mean ± SD (n = 3 independent experiments). $^{\#\#\#}p < 0.001$ vs. Ctr; $^{\Delta\Delta\Delta}p < 0.001$ vs. H_2O_2+shNC+NC; $^{\wedge\wedge\wedge}p < 0.001$ vs. H_2O_2+shEFNB2+NC; $^{\blacktriangle\blacktriangle\blacktriangle}p < 0.001$ vs. H_2O_2+shNC+FTO. EFNB2, ephrin B2; RGCs, retinal ganglion cells; shEFNB2, short hairpin RNA against EFNB2; Ctr, control; H_2O_2, hydrogen peroxide; FTO, fat mass- and obesity-associated gene; ROS, reactive oxygen species; Bax, Bcl-2 associated X; EPHB4, erythropoietin-producing hepatoma receptor B4; NC, Negative Control.

RGC injury by activating the Sirt6-Nrf2/HO-1 signaling pathway [32]. EFNB2, a transmembrane ligand involved in neural development and neuronal migration, is upregulated after optic nerve injury [16,18]. EFNB2 binds EPHB receptors to mediate bidirectional signaling, regulating synaptic plasticity, axon guidance and neurite outgrowth [33]. Through inflammatory pathways in the retina and retinal Müller cells, EPHB1 damages the retina [34]. EPHB/EFNB signaling is upregulated in diabetic retinopathy [35], but the role of EFNB2 in oxidative-injured RGCs remains unclear. Here, H_2O_2 induced EFNB2 expression in a concentration-dependent manner. EFNB2 knockdown exacerbated H_2O_2-mediated reductions in viability and increases in apoptosis, ROS levels, and pro-apoptotic protein expression. These findings suggest that EFNB2 plays a protective role against H_2O_2-induced damage in RGCs.

Among the genes with upregulated m6A methylation, EFNB2, which contained an FTO modification site, was the only gene consistent with our expectation that FTO promotes EFNB2 expression via demethylation [23]. The direct biochemical involvement of m6A demethylation in this specific model requires further experimental verification. FTO, which belongs to the Fe (II)- and alpha-ketoglutarate-dependent (AlkB) dioxygenase family, has been shown to be highly abundant in the brain and closely associated with reduced brain volume in adolescents [36,37]. Also, FTO deficiency has been proven to repress the proliferation and neuronal differentiation of adult neural stem cells [25]. Loss of FTO changes the m6A modification of the transcriptome and plays a regulatory role in neuronal survival, development and activity in the neuronal system [38]. Additionally, the specific and constitutive deletion of FTO is responsible for abnormal adult neurogenesis via the regulation of brain-derived neurotrophic factor (BDNF) and signal transducer and activator of transcription 3 (Stat3) signaling [36,39]. Previous studies have suggested that FTO is of great importance for neuronal activity and function. Moreover, FTO has been demonstrated to be associated with primary open-angle glaucoma [37]. However, FTO may play context-dependent roles in neurological disorders. Previous studies have further reported that FTO can exert neuroprotective effects by regulating oxidative stress and neuronal death [40], whereas dysregulated FTO may also be in-

volved in neuroinflammation, neurotoxicity, and neuronal dysfunction [41,42]. Therefore, the effects of FTO may vary depending on the disease model, cell type, injury stage, and downstream targets.

Although the role of FTO and the FTO-related mechanism of EFNB2 in RGCs are largely unknown, our experimental results show that FTO expression was enhanced by H_2O_2 in a concentration-dependent manner. It is noteworthy that H_2O_2 treatment alone upregulated both FTO and EFNB2, which may reflect an endogenous stress response; however, this endogenous upregulation appeared insufficient to fully protect RGCs against oxidative injury, as FTO overexpression was required to achieve significant protection. FTO overexpression attenuated the H_2O_2-induced decrease in RGC viability, together with an increase in cell apoptosis and caspase-3 activity and ROS level, while upregulating the expression levels of EFNB2/EPHB4 and suppressing Bax and cleaved caspase-3 in RGCs. Additionally, EFNB2 knockdown reversed the effects of FTO on RGC viability, apoptosis, ROS level, and the expression levels of EPHB4, Bax, and cleaved caspase-3. These findings suggest that FTO-mediated protection is associated with the upregulation of EFNB2 expression in RGCs. Furthermore, we speculate that FTO modulation of EFNB2 might serve as a cellular stress response during oxidative injury, though whether this process relies strictly on m6A demethylation remains a hypothesis to be fully tested.

This study has several limitations. First, the experiments were performed *in vitro*; the FTO/EFNB2 axis requires validation in animal models of traumatic optic neuropathy. Second, while we hypothesize that FTO may regulate EFNB2 through m6A demethylation, no direct m6A-related experiments (such as MeRIP-qPCR, m6A quantification, or RNA stability assays) were performed in this study. Finally, the narrow range of H_2O_2 concentrations used in the cytotoxicity assays failed to fully elucidate the dose-effect relationship of oxidative injury.

Conclusions

In summary, this study demonstrates that the FTO/EFNB2 axis protects RGCs against H_2O_2-induced oxidative damage. FTO upregulates EFNB2 and EPHB4 expression, reduces ROS accumulation and apoptosis, and enhances RGC viability. EFNB2 knockdown reverses these protective effects, indicating that EFNB2 functions as a downstream effector of FTO. To the best of our knowledge, this is the first study to implicate EFNB2 in RGC oxidative damage. Although direct evidence for m6A-dependent regulation and EPHB4 signaling activation is lacking, our findings identify the FTO/EFNB2 axis as a potential therapeutic target for oxidative stress-related RGC injury. Future *in vivo* studies and mechanistic investigations are warranted to validate these findings.

Availability of Data and Materials

The datasets used or analyzed during the current study are available from the corresponding authors on reasonable request.

Author Contributions

YY, YZ and ZXX designed the study and drafted the manuscript; YY, YW and BBZ performed the experiments and analyzed the data; ZYM, YZ and ZXX analyzed and interpreted the data. All authors have been involved in revising it critically for important intellectual content. All authors gave final approval of the version to be published. All authors have participated sufficiently in the work to take public responsibility for appropriate portions of the content and agreed to be accountable for all aspects of the work in ensuring that questions related to its accuracy or integrity.

Ethics Approval and Consent to Participate

All experimentation involving animals was conducted in accordance with institutional guidelines for the care and use of laboratory animals and received approval from the Zhejiang Provincial Experimental Animal Center's Experimental Animal Welfare and Ethics Committee (approval No. ZJCLA-IACUC-20140023). All procedures complied with the ARRIVE Guidelines 2.0.

Acknowledgment

Not applicable.

Funding

This research received no external funding.

Conflict of Interest

The authors declare no conflict of interest.

References

[1] Karimi S, Arabi A, Ansari I, Shahraki T, Safi S. A Systematic Literature Review on Traumatic Optic Neuropathy. Journal of Ophthalmology. 2021; 2021: 5553885. https://doi.org/10.1155/2021/5553885

[2] Blanch RJ, Joseph IJ, Cockerham K. Traumatic optic neuropathy management: a systematic review. Eye (London, England). 2024; 38: 2312–2318. https://doi.org/10.1038/s41433-024-03129-7

[3] Bacorn C, Morisada MV, Dedhia RD, Steele TO, Strong EB, Lin LK. Traumatic Optic Neuropathy Management: A Survey Assessment of Current Practice Patterns. Journal of Emergencies, Trauma, and Shock. 2021; 14: 136–142. https://doi.org/10.4103/JETS.JETS_66_20

[4] Lee J, Nguyen S, Bhattacharya S. Optic nerve regeneration: Potential treatment approaches. Current Opinion in Pharmacology. 2024; 74: 102428. https://doi.org/10.1016/j.coph.2023.102428

[5] Meng Z, You R, Mahmood A, Yan F, Wang Y. Application of Proteomics Analysis and Animal Models in Optic Nerve Injury Diseases. Brain Sciences. 2023; 13: 404. https://doi.org/10.3390/brainsci13030404

[6] Ju WK, Perkins GA, Kim KY, Bastola T, Choi WY, Choi SH. Glaucomatous optic neuropathy: Mitochondrial dynamics, dysfunction and protection in retinal ganglion cells. Progress in Retinal and Eye Research. 2023; 95: 101136. https://doi.org/10.1016/j.preteyeres.2022.101136

[7] Espinosa-Diez C, Miguel V, Mennerich D, Kietzmann T, Sánchez-Pérez P, Cadenas S, et al. Antioxidant responses and cellular adjustments to oxidative stress. Redox Biology. 2015; 6: 183–197. https://doi.org/10.1016/j.redox.2015.07.008

[8] Takahashi N, Tawarayama H, Chida Y, Takeda M, Shiokawa R, Sato K, et al. ENO1 Dysfunction-Mediated Glycolytic Attenuation Exacerbates Oxidative Stress-Induced Retinal Ganglion Cell Death via Altered ATP Synthesis Pathway. Investigative Ophthalmology & Visual Science. 2025; 66: 63. https://doi.org/10.1167/iovs.66.9.63

[9] Stockwell BR, Friedmann Angeli JP, Bayir H, Bush AI, Conrad M, Dixon SJ, et al. Ferroptosis: A Regulated Cell Death Nexus Linking Metabolism, Redox Biology, and Disease. Cell. 2017; 171: 273–285. https://doi.org/10.1016/j.cell.2017.09.021

[10] Wang C, Feng L, Fang W, Zhang C, Zhang W, Zhu W, et al. Inhibition of Mettl3-mediated m6A RNA modification of HMGCS1 protects retinal ganglion cells from glutamate excitotoxicity-induced ferroptosis in a rat model of glaucoma. International Journal of Surgery (London, England). 2025; 111: 9147–9165. https://doi.org/10.1097/JS9.0000000000003213

[11] Gao M, Zhou J, Shi N, Yan X, Liang L. Neuroinflammatory regulatory role of microglia in optic nerve injury: from pathological mechanisms to therapeutic targets. Frontiers in Immunology. 2026; 17: 1742677. https://doi.org/10.3389/fimmu.2026.1742677

[12] Wei J, Yu X, Yang L, Liu X, Gao B, Huang B, et al. FTO mediates LINE1 m^6A demethylation and chromatin regulation in mESCs and mouse development. Science (New York, N.Y.). 2022; 376: 968–973. https://doi.org/10.1126/science.abe9582

[13] Koury J, Singh H, Sutley-Koury SN, Fok D, Qiu X, Maung R, et al. EphB2-mediated ephrin-B reverse signaling on microglia drives an anti-viral, but inflammatory and neurotoxic response associated with HIV. Journal of Neuroinflammation. 2025; 22: 171. https://doi.org/10.1186/s12974-025-03481-9

[14] Kakarla M, ChallaSivaKanaka S, Dufficy MF, Gil V, Filipovich Y, Vickman R, et al. Ephrin B Activate Src Family Kinases in Fibroblasts Inducing Stromal Remodeling in Prostate Cancer. Cancers. 2022; 14: 2336. https://doi.org/10.3390/cancers14092336

[15] Rasool D, Jahani-Asl A. Master regulators of neurogenesis: the dynamic roles of Ephrin receptors across diverse cellular niches. Translational Psychiatry. 2024; 14: 462. https://doi.org/10.1038/s41398-024-03168-4

[16] Strong TA, Esquivel J, Wang Q, Ledon PJ, Wang H, Gaidosh G, et al. Activation of multiple Eph receptors on neuronal membranes correlates with the onset of optic neuropathy. Eye and Vision (London, England). 2023; 10: 42. https://doi.org/10.1186/s40662-023-00359-w

[17] David ET, Yousuf MS, Mei HR, Jain A, Krishnagiri S, Elahi H, et al. ephrin-B2 promotes nociceptive plasticity and hyperalgesic priming through EphB2-MNK-eIF4E signaling in both mice and humans. Pharmacological Research. 2024; 206: 107284. https://doi.org/10.1016/j.phrs.2024.107284

[18] Lévy J, Haye D, Marziliano N, Casu G, Guimiot F, Dupont C, et al. EFNB2 haploinsufficiency causes a syndromic neurodevelopmental disorder. Clinical Genetics. 2018; 93: 1141–1147. https://doi.org/10.1111/cge.13234

[19] Li X, Ma B, Zhang W, Song Z, Zhang X, Liao M, et al. The essential role of N6-methyladenosine RNA methylation in complex eye diseases. Genes & Diseases. 2023; 10: 505–520. https://doi.org/10.1016/j.gendis.2022.05.008

[20] Wan W, Ao X, Chen Q, Yu Y, Ao L, Xing W, et al. METTL3/IGF2BP3 axis inhibits tumor immune surveillance by upregulating N^6-methyladenosine modification of PD-L1 mRNA in breast cancer. Molecular Cancer. 2022; 21: 60. https://doi.org/10.1186/s12943-021-01447-y

[21] Chen XY, Zhang J, Zhu JS. The role of m^6A RNA methylation in human cancer. Molecular Cancer. 2019; 18: 103. https://doi.org/10.1186/s12943-019-1033-z

[22] Qiu J, Zhao R, Ma C, Wang Q, Li B, Qi Y, et al. O-GlcNAcylation stabilized WTAP promotes GBM malignant progression in an N6-methyladenosine-dependent manner. Neuro-oncology. 2025; 27: 900–915. https://doi.org/10.1093/neuonc/noae268

[23] Qi Z, Wang S, Li J, Wen Y, Cui R, Zhang K, et al. Protective role of mRNA demethylase FTO on axon guidance molecules of nigro-striatal projection system in manganese-induced parkinsonism. Journal of Hazardous Materials. 2022; 426: 128099. https://doi.org/10.1016/j.jhazmat.2021.128099

[24] Jiang J, Zhang M, Xia W, Ding C, Li J, Hu X, et al. Fto-mediated m^6A modification is essential for cerebellar development through regulating epigenetic reprogramming. Journal of Biomedical Science. 2025; 32: 81. https://doi.org/10.1186/s12929-025-01176-0

[25] Li L, Zang L, Zhang F, Chen J, Shen H, Shu L, et al. Fat mass and obesity-associated (FTO) protein regulates adult neurogenesis. Human Molecular Genetics. 2017; 26: 2398–2411. https://doi.org/10.1093/hmg/ddx128

[26] Azcoitia I, Barreto GE, Garcia-Segura LM. Molecular mechanisms and cellular events involved in the neuroprotective actions of estradiol. Analysis of sex differences. Frontiers in Neuroendocrinology. 2019; 55: 100787. https://doi.org/10.1016/j.yfrne.2019.100787

[27] Meyer-Franke A, Kaplan MR, Pfrieger FW, Barres BA. Characterization of the signaling interactions that promote the survival and growth of developing retinal ganglion cells in culture. Neuron. 1995; 10: 805–819. https://doi.org/10.1016/0896-6273(95)90172-8

[28] Mueller-Buehl AM, Doepper H, Grauthoff S, Kiebler T, Peters L, Hurst J, et al. Oxidative stress-induced retinal damage is prevented by mild hypothermia in an ex vivo model of cultivated porcine retinas. Clinical & Experimental Ophthalmology. 2020; 48: 666–681. https://doi.org/10.1111/ceo.13731

[29] Livak KJ, Schmittgen TD. Analysis of relative gene expression data using real-time quantitative PCR and the 2(-Delta Delta C(T)) Method. Methods (San Diego, Calif.). 2001; 25: 402–408. https://doi.org/10.1006/meth.2001.1262

[30] Hahn J, Monavarfeshani A, Qiao M, Kao AH, Kölsch Y, Kumar A, et al. Evolution of neuronal cell classes and types in the vertebrate retina. Nature. 2023; 624: 415–424. https://doi.org/10.1038/s41586-023-06638-9

[31] Buonfiglio F, Böhm EW, Pfeiffer N, Gericke A. Oxidative Stress: A Suitable Therapeutic Target for Optic Nerve Diseases? Antioxidants (Basel, Switzerland). 2023; 12: 1465. https://doi.org/10.3390/antiox12071465

[32] Yu JN, Wang SM, Liu JR, Xue F, Yang XG, Lv ZY. Crocin Protects Against Retinal Ischemia-Reperfusion Injury via Regulating Sirt6-Mediated Nrf2/HO-1 Pathway in Rats. Investigative Ophthalmology & Visual Science. 2026; 67: 23. https://doi.org/10.1167/iovs.67.1.23

[33] Kaur S, Bali A, Singh N, Jaggi AS. Ephrin B/EphB in neuropathic pain: Role and molecular mechanisms. Fundamental & Clinical Pharmacology. 2024; 38: 4–12. https://doi.org/10.

1111/fcp.12937

[34] Liu L, Jiang Y, Al-Shabrawey M, Ren X, Wang S, Steinle JJ. EphB1 causes retinal damage through inflammatory pathways in the retina and retinal Müller cells. Molecular Vision. 2024; 30: 167–174.

[35] Roskoski R, Jr. Vascular endothelial cells and angiogenesis. Pharmacological Research. 2025; 221: 107983. https://doi.org/10.1016/j.phrs.2025.107983

[36] Irisarri A, Corral A, Perez-Salvador N, Bellver-Sanchis A, Ribalta-Vilella M, Bentanachs R, et al. FTO inhibition mitigates high-fat diet-induced metabolic disturbances and cognitive decline in SAMP8 mice. Molecular Medicine (Cambridge, Mass.). 2025; 31: 73. https://doi.org/10.1186/s10020-025-01126-4

[37] Abbas S, Raza ST, Chandra A, Singh L, Mahdi F. Association of fatty acid-binding protein 2 and fat mass and obesity-associated gene polymorphism with primary open-angle glaucoma. Taiwan Journal of Ophthalmology. 2017; 7: 138–142. https://doi.org/10.4103/tjo.tjo_10_17

[38] Hao J, Yang Y, Xie L, Li Z, Ma B, Wang B, et al. Actl6a regulates autophagy via Sox2-dependent Atg5 and Atg7 expression to inhibit apoptosis in spinal cord injury. Journal of Advanced Research. 2025; 77: 281–296. https://doi.org/10.1016/j.jare.2025.01.038

[39] Cao Y, Zhuang Y, Chen J, Xu W, Shou Y, Huang X, et al. Dynamic effects of Fto in regulating the proliferation and differentiation of adult neural stem cells of mice. Human Molecular Genetics. 2020; 29: 727–735. https://doi.org/10.1093/hmg/ddz274

[40] Hou L, Li S, Li S, Wang R, Zhao M, Liu X. FTO inhibits oxidative stress by mediating m6A demethylation of Nrf2 to alleviate cerebral ischemia/reperfusion injury. Journal of Physiology and Biochemistry. 2023; 79: 133–146. https://doi.org/10.1007/s13105-022-00929-x

[41] Song J, Hao J, Lu Y, Ding X, Li M, Xin Y. Increased m^6A modification of BDNF mRNA via FTO promotes neuronal apoptosis following aluminum-induced oxidative stress. Environmental Pollution (Barking, Essex : 1987). 2024; 349: 123848. https://doi.org/10.1016/j.envpol.2024.123848

[42] Zhou T, Zhou R, Jiang X, Gao Y, Zhang J, Zhou L, et al. m^6A modification of ATG9A regulates ferritinophagy in microglial activation induced by arsenic. Journal of Hazardous Materials. 2025; 496: 139376. https://doi.org/10.1016/j.jhazmat.2025.139376